J. Fluid Mech. (1995), *vol.* 293, *pp.* 181–206

The effect of blade sweep on the reduction and enhancement of supersonic propeller noise

By A. B. PARRY†

Department of Mathematics, University of Strathclyde, Glasgow G1 1XH, UK

(Received 13 March 1994 and in revised form 27 January 1995)

An asymptotic frequency-domain approach is used to describe the radiation from a supersonic swept propeller within the framework of linear acoustics. With this approach the radiation of singularities, their points of origin on the blades, and their relation to blade geometry and loading are easily obtained. In particular, it is shown that a swept propeller with a completely subsonic leading edge can still radiate singularities, if the leading edge is blunt, due to a supersonic edge effect at the blade tips. In addition, the radiation from a family of 'critical' swept-blade designs is shown to be more singular than that from a straight-bladed design. Numerical and asymptotic results for such designs show that the peak radiation is, typically, increased by 5–10 dB.

1. Introduction

The advanced propellers currently being studied generally incorporate some degree of blade sweep (see, particularly, Metzger & Rohrbach 1979, 1985). Sweep is included in the blade design mainly for aerodynamic reasons but, in addition, it also produces acoustic benefits because the signals, emitted from different radial stations, are partially dephased. Some discussion of this aspect has been given by Hanson (1980*a*).

When linear theory is used to predict the radiation from propellers operating supersonically it is found (Hawkings & Lowson 1974; Tam 1983; Amiet 1988; Chapman 1988) that singularities are present in the pressure field. All previous work of this nature, with the exception of Amiet (1988), has concentrated solely on straight-bladed propellers. As will be shown, however, the swept-blade case throws up a number of extremely interesting possibilities – none of which can occur on a straight-bladed design – of some concern for enhanced noise radiation.

Amiet (1988) carried out a full time-domain analysis suggesting, first, that this gives a more physical understanding of the singularities and their point of origin on the blade – with a frequency-domain approach, he argued, it becomes difficult to determine detailed source locations – and second that, if the results of the frequency domain are inverted back to the time domain, the singular peaks and abrupt slope changes in the pressure–time waveform will require many frequency terms to get comparable resolution. Amiet showed that the singularities were radiated from regions on the blade edges that move towards the observer at sonic speed while at the same time having the edge normal to the line joining the source point and the observer. Accordingly, he concluded that the singularities can be removed by sweeping the rotors so that the Mach number component normal to the leading and trailing edges is subsonic for all points on the rotor edges. The limitations of Amiet's work are, however, that the blade leading- and trailing-edge shapes are fixed (sharp or, more precisely, wedge-shaped) and that the noise source is restricted to thickness noise.

† Now at Rolls-Royce plc, PO Box 31, Derby DE24 8BJ, UK.

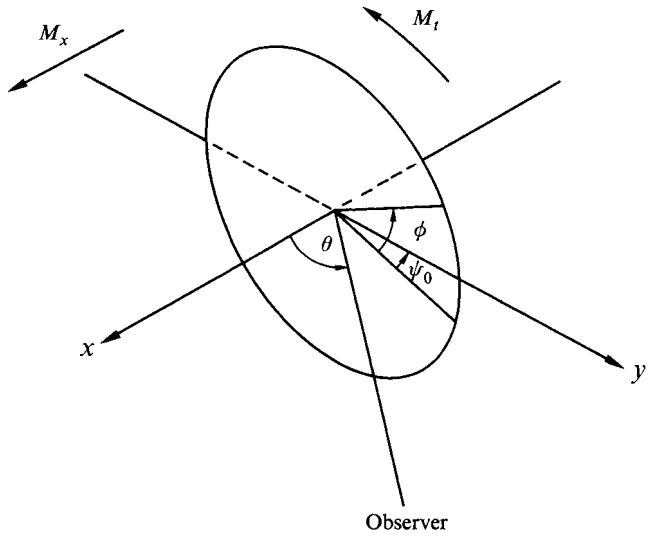

FIGURE 1. The nominal propeller disk plane.

Here we use an asymptotic far-field frequency-domain approach, valid in the limit $mB \to \infty$, where B is the number of blades and m is the harmonic of blade passing frequency. Previous work (Parry & Crighton 1989; Crighton & Parry 1991, 1992) has shown the accuracy of this approach – even at relatively low values of mB. The noise radiation, in the frequency domain, can be put in the form of a triple source integral: an integral along the blade chord between leading edge and trailing edge; an integral along the blade span between hub and tip; and an azimuthal integral around the nominal propeller disk. The latter integral, however, can be evaluated analytically producing the usual Bessel function (see, for example, Hanson 1980*b*). The radial integral can, therefore, be evaluated asymptotically using an appropriate form for the Bessel function and the properties of one-dimensional integrals (the chordwise integral being incorporated into a spanwise source term).

For the case of a swept propeller it is preferable to retain the azimuthal integral, as did Hawkings & Lowson (1974), and carry out the analysis using asymptotics of double integrals (see, for example, Jones & Kline 1959; Chako 1965; Bleistein & Handelsman 1969; Dingle 1973, chap. IX); with this approach we can obtain not only the radial stations from which singularities are radiated, but also the azimuthal angle, i.e. we do, indeed, obtain the detailed source locations. In addition, the asymptotic frequency-domain approach gives us, automatically, the precise dependence of the high-frequency components on mB; we can thus determine, immediately, the form of any radiated singularity. We thus argue that the asymptotic frequency-domain approach can generate an enhanced understanding of the underlying physical noise-generating mechanisms, as well as producing remarkably simplified, and accurate, formulae for noise generation.

In §2 we use stationary phase techniques for double integrals to show that, in agreement with Amiet (1988), the radiation is dominated by contributions from regions on the blade edges that move towards the observer at sonic speed whilst having the edge normal to the line joining the source point and the observer. The presence of singular radiation is discussed in §3 along with the relation between the form of the singularity and the details of blade loading and geometry. In §4 we examine Amiet's 'minimum sweep' concept and discuss radiation from propellers with completely

subsonic leading edges. The precise origin of the singular radiation, in terms of radii and azimuth, is presented in §5. In §6 we discuss the possibilities of enhanced noise radiation and calculate the shapes of a family of 'critical' designs. Comparisons between numerical and asymptotic results are given in §7 for swept propellers with subsonic, transonic and supersonic leading edges. Conclusions are presented in §8.

2. The leading-order solution

2.1. *Background*

Crighton & Parry (1991) have shown that for a straight-bladed propeller operating supersonically the far-field radiation in direction θ is dominated by that section of the blade, $z = z^*$, which approaches the observer at θ with precisely sonic speed; provided, of course, that θ lies in the range for which $M_o(\theta) = M_t \sin\theta + M_x \cos\theta$, the tip Mach number component resolved in the direction θ, is greater than unity. Here, θ represents the angle between the propeller flight axis and a line drawn from the centre of the propeller to the observer, z denotes a blade element radius, normalized by the blade tip radius, and M_t and M_x are the propeller tip rotational and axial Mach numbers respectively (see figure 1). The 'straight-blade' Mach radius is given by

$$z^* = (1 - M_x \cos\theta)/(M_t \sin\theta). \tag{1}$$

For the present we neglect the effects of chordwise non-compactness so that the harmonic components of the far-field radiated sound are given by (Parry & Crighton 1989; Crighton & Parry 1991, 1992)

$$P_m = \int_{z_0}^{1} S(z)\, J_{mB}(mB\, z/z^*)\, \mathrm{e}^{-\mathrm{i}\phi_s}\, \mathrm{d}z, \tag{2}$$

where, as usual, $S(z)$ is used generically to denote the source strength at radial station z and ϕ_s is a phase term, introduced by Hanson (1980*b*)†, representing the effects of blade sweep, defined by

$$\phi_s = \frac{2mBM_t\, s/D}{M_r(1 - M_x \cos\theta)}, \tag{3}$$

and z_0 is the propeller hub/tip ratio. The sweep parameter s is, in common with Hanson (1980*a*) and Amiet (1988), the distance the blade is swept back along the helical path it describes, D is the propeller diameter and $M_r = (M_x^2 + z^2 M_t^2)^{1/2}$ is the blade-section relative Mach number. The full waveform, as a function of time, is obtained from (2) by introducing the amplitude and phase multiplying factors and summing the harmonics:

$$p(t) = \frac{-\rho c_0^2 DB}{8\pi r_0 (1 - M_x \cos\theta)} \sum_{m=-\infty}^{\infty} \exp\left[\frac{\mathrm{i}mB\Omega}{(1 - M_x \cos\theta)}\left(t - \frac{r_0}{c_0}\right) + \mathrm{i}mB\left(\tfrac{1}{2}\pi - \psi_0\right)\right] P_m. \tag{4}$$

In (4) ρ is density, c_0 is the ambient speed of sound, r_0 is the distance from the centre of the propeller to the observer, Ω is the shaft angular speed and ψ_0 is the circumferential angle between the observer and the reference position. The source strength term in (2) is given by

$$S(z) = \mathrm{i}k_y (C_L/2) M_r^2, \quad S(z) = k_x^2 (b/c) M_r^2 \tag{5}$$

† Note that, as in earlier papers, our expressions are, essentially, the complex conjugates of Hanson's since he assumed a time dependence $\mathrm{e}^{-\mathrm{i}\omega t}$ and we have used $\mathrm{e}^{\mathrm{i}\omega t}$.

for the blade loading and thickness source terms respectively, where the non-dimensional wavenumbers k_x and k_y are defined by

$$k_x = \frac{2mBM_t c/D}{M_r(1-M_x\cos\theta)}, \tag{6}$$

$$k_y = \frac{2mB(M_r^2\cos\theta - M_x)\, c/D}{zM_r(1-M_x\cos\theta)}, \tag{7}$$

C_L is the blade-section lift coefficient, b is the maximum section thickness and c is the local chord length. We thus note the dependence of $S(z)$ on the observer position θ, the forward and rotational Mach numbers M_x and M_t, and on the harmonic product mB. We will see later that this latter dependence is important in determining the significant physical characteristics of noise radiation.

2.2. *Stationary phase*

We now need to tackle the integral (2) in the limit $mB \to \infty$. The most appropriate way to do this is by introducing the integral form of the Bessel function,

$$J_{mB}\left(mB\frac{z}{z^*}\right) = \frac{1}{2\pi \mathrm{i}^{mB}}\int_{-\pi}^{\pi} \exp\left[\mathrm{i}mB\left(t+\frac{z}{z^*}\cos t\right)\right]\mathrm{d}t \tag{8}$$

(here, and throughout the remainder of the paper, t is taken to be a dummy integration variable), so that (2) is written as the double integral

$$P_m = \frac{1}{2\pi \mathrm{i}^{mB}}\int_{z_0}^{1}\int_{-\pi}^{\pi} S(z)\exp\left[\mathrm{i}mBf(z,t)\right]\mathrm{d}t\,\mathrm{d}z, \tag{9}$$

where

$$f(z,t) = t + (z/z^*)\cos t - \psi_s(z), \tag{10}$$

and the modified sweep phase factor is

$$\psi_s(z) = \frac{M_t\bar{s}}{M_r(1-M_x\cos\theta)}. \tag{11}$$

Here, for simplicity, we have introduced a normalized sweep parameters $\bar{s} = 2s/D$. The double integral (9) can then be evaluated in the limit $mB \to \infty$ using the method of stationary phase in two dimensions (see, for example, Chako 1965). The first- and second-order partial derivatives of $f(z,t)$ are needed throughout the work that follows. We thus list them here as

$$\left.\begin{aligned} &\frac{\partial f}{\partial z} = \frac{\cos t}{z^*} - \psi_s'(z), \quad \frac{\partial f}{\partial t} = 1 - \frac{z}{z^*}\sin t, \\ &\frac{\partial^2 f}{\partial z^2} = -\psi_s''(z), \quad \frac{\partial^2 f}{\partial z\,\partial t} = -\frac{\sin t}{z^*}, \quad \frac{\partial^2 f}{\partial t^2} = -\frac{z}{z^*}\cos t, \end{aligned}\right\} \tag{12}$$

so that at a stationary point (or, following Chako 1965, an interior critical point), where $\partial f/\partial z = \partial f/\partial t = 0$, we have

$$\cos t = z^*\psi_s'(z), \quad \sin t = z^*/z \tag{13}$$

or, on eliminating t,

$$z^{*2}\{[\psi_s'(z)]^2 + 1/z^2\} = 1. \tag{14}$$

We assume, for the present, that the solution to (14), $z = \tilde{z}$ say, lies on the blade†, i.e. $z_0 < \tilde{z} < 1$. (Of course, when, $\psi_s(z) = 0$ we obtain simply $z = z^*$, the 'straight-blade' Mach radius.) Expanding $f(z, t)$ and $S(z)$ in a Taylor series about $z = \tilde{z}$, $t = \tilde{t}$ (where $t = \tilde{t}$ is the solution of (13) at $z = \tilde{z}$), we obtain the leading-order contribution from the stationary phase point as

$$P_m \sim \frac{S(\tilde{z})\,\mathrm{e}^{\mathrm{i}mBf_{0,0}}}{2\pi \mathrm{i}^{mB}} \int_{-\infty}^{\infty}\int_{-\infty}^{\infty} \exp\left\{\frac{\mathrm{i}mB}{2}\left[\left(f_{2,0} - \frac{f_{1,1}^2}{f_{0,2}}\right)Z^2 + f_{0,2}T^2\right]\right\} \mathrm{d}T\,\mathrm{d}Z, \tag{15}$$

where we have introduced the notation

$$f_{j,k} = \frac{\partial^{j+k}}{\partial^j z\,\partial^k t} f(\tilde{z}, \tilde{t}) \tag{16}$$

and used the simple transformation

$$Z = z - \tilde{z}, \quad T = (t - \tilde{t}) + \frac{f_{1,1}}{f_{0,2}}(z - \tilde{z}), \tag{17}$$

for which the Jacobian is unity. The integral is easily evaluated as

$$P_m \sim \frac{S(\tilde{z})}{|mB|\,|f_{2,0}f_{0,2} - f_{1,1}^2|^{1/2}} \times \exp\{\mathrm{i}mB(f_{0,0} - \tfrac{1}{2}\pi) + \mathrm{i}\tfrac{1}{4}\pi\,\mathrm{sgn}\,(mB)\,\mathrm{sgn}\,(f_{0,2})\,[1 + \mathrm{sgn}\,(f_{2,0}f_{0,2} - f_{1,1}^2)]\}. \tag{18}$$

In the straight-bladed case it is easy to see from (13) that $\tilde{z} = z^*$ and $\tilde{t} = \pi/2$ so that (18) reduces to

$$P_m \sim z^* S(z^*)/|mB|. \tag{19}$$

This result was given previously in Crighton & Parry (1991) where it was observed that, when taken in conjunction with the shape of the blade leading and trailing edges (i.e. blunt, wedge-shaped or cusp-shaped), or the form of the chordwise blade loading distribution near the leading and trailing edges, (19) could indicate, immediately, the type of singularity radiated from the Mach radius towards the observer.

In the swept case we can see clearly that, provided the solution $z = \tilde{z}$ to (14) lies on the blade, the leading term of the solution is of the same order as that in the straight-blade case.

2.3. *The 'swept-blade' Mach radius*

It is, of course, important to understand where precisely $\tilde{z}$ lies on the blade and whether this point has any physical significance. Indeed, we need to compare our result with that of Amiet (1988) who showed that, for the specific case of an airfoil with sharp leading and trailing edges (or, more precisely wedge-shape leading and trailing edges), logarithmic singularities in the waveform are produced by regions on the blade edges that move towards the observer at sonic speed while at the same time having the edge normal to the line joining the sonic point and the observer.

To make this comparison we follow Amiet (1988) and introduce a local blade sweep angle Λ where the blade is projected onto a plane (the nominal propeller disk) which is normal to the axis of translation, with Λ defined as the angle between the radius

† As will become clear later, there is, potentially, more than one solution to (14).

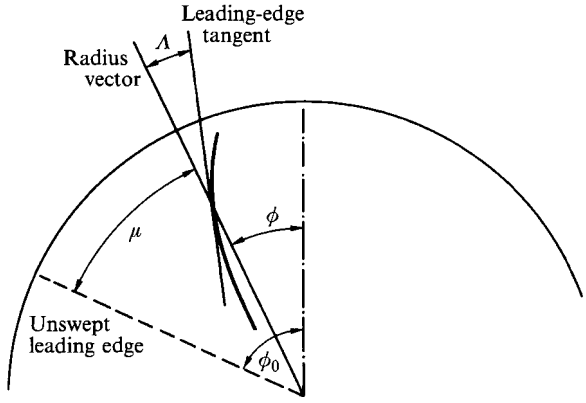

FIGURE 2. The blade swept and unswept leading-edge geometries in the nominal disk plane.

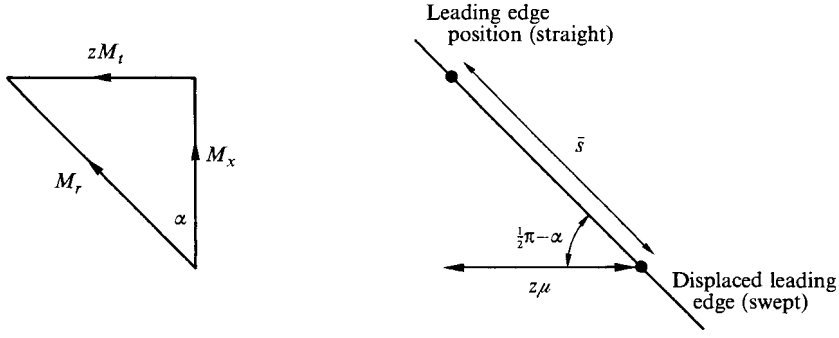

FIGURE 3. Mach number triangle and its relation to the displaced leading-edge position.

vector and the tangent to the leading edge (see figure 2). Then, Λ can be related to the variation in the propeller azimuth with radius by

$$\tan\Lambda = -z\,\mathrm{d}\phi/\mathrm{d}z, \tag{20}$$

where $\phi = \phi_0 - \mu$. The reference axis $\phi = \phi_0$ represents the unswept leading edge. Since the propeller is swept back along the helical path it describes, we can use the Mach number triangle (see figure 3) to obtain

$$\mu = (\bar{s}\sin\alpha)/z, \quad \sin\alpha = zM_t/M_r, \tag{21}$$

where α is the local blade stagger angle; a helical sweep of $\bar{s}$ thus corresponds to an azimuthal displacement of $z\mu$. From (11) and (21) we see that μ is related to the sweep phase factor ψ_s by

$$\mu = (1 - M_x\cos\theta)\,\psi_s(z), \tag{22}$$

so that, on differentiating with respect to z and using (20), we obtain

$$\psi_s'(z) = \frac{\tan\Lambda}{z(1 - M_x\cos\theta)}. \tag{23}$$

Equation (14), which determines the radial station(s) providing the leading-order contribution(s) to the radiated sound, thus becomes $\tan^2\Lambda/[z^2(1 - M_x\cos\theta)^2] + 1/z^2 = 1/z^{*2}$ or, on replacing the 'straight-blade' Mach radius from (1),

$$\tan^2\Lambda + (1 - M_x\cos\theta)^2 = M_t^2 z^2 \sin^2\theta. \tag{24}$$

It is easiest to interpret this equation for the case of a propeller with no translation, i.e. $M_x = 0$. Then (24) reduces to

$$zM_t \cos\Lambda \sin\theta = 1. \tag{25}$$

We consider, as in previous papers, an observer in the far field positioned, without loss of generality, in a horizontal plane through the propeller axis. It is clear that the solution $z = \tilde{z}$ to (25) represents a point on the blade where the Mach number component normal to the leading edge is sonic in the direction of an observer at θ.

We now consider the case of a translating propeller, i.e. $M_x \neq 0$, by introducing x, y coordinates where the x-axis coincides with the propeller axis and the y-axis is normal to the x-axis and lies in a horizontal plane; the origin of coordinates is at the centre of the nominal propeller disk. For a specific blade, such as that described in figures 1 and 2, the position of the leading edge at radial station z, in terms of x and y, is

$$x = -\bar{s}\cos\alpha = -\bar{s}\frac{M_x}{M_r} = -\frac{M_x}{M_t}(1 - M_x\cos\theta)\,\psi_s(z), \quad y = z\cos\phi. \tag{26}$$

Note that here, and in what follows, we take ϕ to be measured from the positive y-axis. On differentiating we find that elemental changes in these coordinates with increasing radius are given by

$$\left.\begin{aligned} \mathrm{d}x/\mathrm{d}z &= -M_x/M_t\,(1 - M_x\cos\theta)\,\psi_s'(z) = -(M_x/zM_t)\tan\Lambda, \\ \mathrm{d}y/\mathrm{d}z &= \cos\phi - z\sin\phi\,\mathrm{d}\phi/\mathrm{d}z = \cos\phi + \sin\phi\tan\Lambda. \end{aligned}\right\} \tag{27}$$

We consider a line from the blade to an observer at θ. This line, of length R, is normal to the leading edge when $\mathrm{d}R/\mathrm{d}z = 0$ or, in terms of x and y, when

$$\cos\theta\,\mathrm{d}x/\mathrm{d}z + \sin\theta\,\mathrm{d}y/\mathrm{d}z = 0. \tag{28}$$

(This analysis is, of course, only valid for an observer in the far field.) Combining (27) and (28) we find that the blade is moving normal to itself in the direction of an observer at θ when

$$-(M_x/zM_t)\tan\Lambda\cos\theta + \cos\phi\sin\theta + \sin\phi\tan\Lambda\sin\theta = 0. \tag{29}$$

We now determine the speed, or Mach number M_{obs}, of this blade in the direction of the observer. For an element at radial station z, positioned at angle ϕ to the horizontal, as in figure 1, this speed is

$$M_{obs} = -zM_t\sin\phi\sin\theta + M_x\cos\theta. \tag{30}$$

The azimuthal angle at which the blade edge is moving towards the observer at precisely sonic speed, therefore, is given by

$$\sin\phi = -(1 - M_x\cos\theta)/(zM_t\sin\theta). \tag{31}$$

Substituting this in (29) we obtain, after a little manipulation, the result $\tan^2\Lambda + (1 - M_x\cos\theta)^2 = z^2M_t^2\sin^2\theta$ – which is precisely the solution obtained using the stationary phase procedure – when the blade edge is travelling normal to itself, at precisely sonic speed, in the direction of an observer at θ.

We have found, therefore, that the radiation from the blade is, to leading order in mB, given by (18) and is dominated, in the general case†, by the contributions from the radial station $z = \tilde{z}$ at which the blade moves normal to itself, and directly towards the observer, at sonic speed. We will, therefore, call $z = \tilde{z}$ the 'swept-blade' Mach radius.

† Situations in which (18) is not the leading-order term, or in which the dominant contribution does not come from the 'swept-blade' Mach radius, will be discussed later.

Amiet (1988) found that, for a wedge-shaped leading edge, logarithmic singularities were radiated, in the thickness-noise sound field, from $z = \tilde{z}$. In order to determine the precise form of the singularities radiated from the leading and trailing edges using the asymptotic frequency-domain approach we proceed, as before (Crighton & Parry 1991), to consider chordwise non-compactness effects.

3. Singularities radiated from the 'swept-blade' Mach radius

3.1. *The general case*

The different types of singularities radiated from the Mach radius have been discussed previously in the context of an asymptotic frequency-domain approach by Crighton & Parry (1991). Here we summarize briefly their results with appropriate modifications being made where necessary to include the effects of blade sweep. The reader is referred to their work for a more detailed description.

In order to consider the effects of blade shape on thickness noise, and of chordwise loading distribution on loading noise, we modify the integrand in (2) by the multiplying factor

$$\Psi(k_x) = \int_{-1/2}^{1/2} F(X)\, \mathrm{e}^{-\mathrm{i}k_x X}\, \mathrm{d}X, \tag{32}$$

where $F(X)$ is a general chordwise shape function corresponding either to the blade loading distribution or the blade thickness distribution. Now k_x is, from (6), proportional to mB so that in the limit $mB \to \infty$ (32) can be evaluated using asymptotic Fourier transform procedures (see, for example, Lighthill 1958). In the region of the blade leading (L) and trailing (T) edges we put

$$\begin{aligned} F(X) &\sim \alpha_L(\tfrac{1}{2}+X)^{\nu_L} \quad \text{as} \quad X \to -\tfrac{1}{2}, \\ \mathrm{F(X)} &\sim \alpha_T(\tfrac{1}{2}-X)^{\nu_T} \quad \text{as} \quad X \to +\tfrac{1}{2}. \end{aligned} \tag{33}$$

We will refer to ν_L and ν_T as the leading- and trailing-edge source gradient orders. Then, as in Crighton & Parry (1991), the chordwise non-compactness factor can be evaluated asymptotically as

$$\Psi(k_x) \sim \frac{\alpha_L \nu_L!}{|k_x|^{\nu_L+1}} \exp\left[\mathrm{i}\frac{k_x}{2} - \mathrm{i}\tfrac{1}{2}\pi(\nu_L+1)\operatorname{sgn}(mB)\right] + \frac{\alpha_T \nu_T!}{|k_x|^{\nu_T+1}} \exp\left[-\mathrm{i}\frac{k_x}{2} + \mathrm{i}\tfrac{1}{2}\pi(\nu_T+1)\operatorname{sgn}(mB)\right]. \tag{34}$$

Accordingly we consider separately the leading-edge and trailing-edge contributions and define a new leading-edge source strength term

$$S_L(z) = \frac{\alpha_L \nu_L!}{|k_x|^{\nu_L+1}} S(z) \exp\left[-\mathrm{i}\tfrac{1}{2}\pi(\nu_L+1)\operatorname{sgn}(mB)\right]. \tag{35}$$

The additional phase term $k_x/2$ in the leading-edge contribution to (34) is accounted for by introducing the normalized leading-edge sweep $s_L = 2(s-c/2)/D$ so that the sweep is now measured from the airfoil leading edge as in Amiet (1988), instead of the pitch change axis as in Hanson (1980*b*) and Crighton & Parry (1991). The sweep phase factor is, accordingly, modified to

$$\psi_L = \frac{M_t s_L}{M_r(1-M_x\cos\theta)}. \tag{36}$$

Similarly, we introduce a new source strength $S_T(z)$ and phase factor ψ_T, with trailing-edge sweep s_T, to represent the trailing-edge contribution.

We can now use the results obtained above to deduce, from the asymptotic form of the harmonic series, the type of singularity radiated from the 'swept-blade' Mach radius. The method is described in detail in the appendix of Crighton & Parry (1991).

3.2. *Thickness noise*

The source strength term $S(z)$ is defined in (5). Since we are, at this stage, only interested in the form of the singularity – or otherwise – radiated from the blade we consider only the amplitude terms related to mB so that

$$S(z) \sim k_x^2 \sim |mB|^2. \tag{37}$$

We now add the effects of chordwise non-compactness as given in (35). Here we consider only the contribution from the leading edge; the trailing-edge contribution can, of course, be treated in an identical manner. An additional term in mB arises from the stationary phase point in the spanwise integral and, from (12) and (18), we are left with

$$\begin{aligned} P_m &\sim \frac{\tilde{z}S(\tilde{z})}{|\tilde{z}^3\psi_s'(\tilde{z})\,\psi_s''(\tilde{z})-1|\,|mB|\,|k_x|^{\nu_L+1}}\exp\left[-\mathrm{i}\tfrac{1}{2}\pi(\nu_L+1)\operatorname{sgn}(mB)\right] \\ &\sim |mB|^{-\nu_L}\{\cos\left[\tfrac{1}{2}\pi(\nu_L+1)\right]-\mathrm{i}\operatorname{sgn}(mB)\sin\left[\tfrac{1}{2}\pi(\nu_L+1)\right]\}. \end{aligned} \tag{38}$$

The additional phase factors in (18) due to blade sweep effects merely serve to shift the origin of any radiated singularities, and to modify the arguments of the sine and cosine terms. The main effect of blade sweep, for a supersonic leading edge, is seen to be represented by the amplitude factor $|\tilde{z}^3\psi_s'(\tilde{z})\,\psi_s''(\tilde{z})-1|^{-1}$; the nature of any radiated singularity thus remains unchanged.

We consider three general cases corresponding to different values of the source gradient order ν_L. If the airfoil has a blunt leading edge then $0 < \nu_L < 1$ so that, on inverting the harmonic series using the methods of Lighthill (1958), we find that weak algebraic singularities of the form $|t|^{-(1-\nu_L)}$ and $\operatorname{sgn}(t)\,|t|^{-(1-\nu_L)}$ are radiated. For the specific case of an airfoil with a parabolic leading edge the thickness varies as $(\frac{1}{2}+X)^{1/2}$ near the edge so that $\nu_L = \frac{1}{2}$; the inverted series thus contains singular terms of the form $|t|^{-1/2}$ and $\operatorname{sgn}(t)\,|t|^{-1/2}$ – it is shown in Crighton & Parry (1991) that these terms actually combine to produce singular terms of the form $[1+\operatorname{sgn}(t)]\,|t|^{-1/2}$. This $|mB|^{-1/2}$ and $|t|^{-1/2}$ behaviour for thickness noise generated by a round leading edge is in agreement with the results of Tam (1983) who considered thickness noise generated by transonic straight-bladed helicopter rotors. The second general case arises when the airfoil has a wedge-shaped leading edge, i.e. the thickness varies as $(\frac{1}{2}+X)$ near the edge. Then $\nu_L = 1$ and the harmonic series produces a waveform containing logarithmic singularities. This result has been found previously by Amiet (1988) who considered thickness noise generated by both straight and swept supersonic propeller blades; it was also mentioned by Tam (1983) whose blades had wedge-shaped trailing edges. Finally, we consider an airfoil with a cusp-shaped leading edge, i.e. the thickness varies as $(\frac{1}{2}+X)^{\nu_L}$ near the edge with $\nu_L > 1$. In the time domain we thus obtain a smooth waveform containing terms of the form $|t|^{\nu_L-1}$ and $\operatorname{sgn}(t)\,|t|^{\nu_L-1}$.

3.3 *Loading noise*

We now turn to the loading noise source and consider whether or not this source term produces singularities in the radiated acoustic pressure. The loading noise case is of particular interest since the recent discussion of radiated singularities in the literature

has been confined to the thickness noise source. The source strength in (5) for blade loading gives

$$S(z) \sim k_y \sim mB = |mB| \operatorname{sgn}(mB). \tag{39}$$

Combining this with (35), representing non-compactness effects, and (18), representing the leading-order contribution from the stationary point, produces harmonic components of the form

$$P_m \sim |mB|^{-\nu_L - 1} \{\operatorname{sgn}(mB) \cos[\tfrac{1}{2}\pi(\nu_L + 1)] - \mathrm{i} \sin[\tfrac{1}{2}\pi(\nu_L + 1)]\}. \tag{40}$$

Here we also consider three general cases corresponding to different values of the source gradient order ν_L. The first of these is the highly loaded leading edge at which the loading is weakly singular, i.e. the loading varies as $(\frac{1}{2}+X)^{\nu_L}$ near the edge with $-1 < \nu_L < 0$. Then, on inverting the harmonic series, we find that weak algebraic singularities of the form $|t|^{\nu_L}$ and $\operatorname{sgn}(t)|t|^{\nu_L}$ are radiated. Secondly, we consider airfoils with finite leading-edge loading, i.e. the loading is constant (to a first approximation) near the edge so that the source gradient order $\nu_L = 0$. The waveform thus contains logarithmic singularities identical to those generated by the thickness noise from a wedge-shaped leading edge. Finally, we consider a lightly loaded leading edge, i.e. the loading approaches zero at the leading edge so that the source gradient order $\nu_L > 0$. Then, as for the thickness noise from a cusp-shaped leading edge, we obtain a smooth radiated pressure field.

4. Removal of the leading-order term

4.1. *Amiet's 'minimum sweep'*

Since the inverse square root and/or logarithmic singularities discussed in §3 emanate from the Mach radius it is, of course, possible to remove them by ensuring that the blade leading and trailing edges are subsonic across the entire span of the blade. This has been discussed previously by Amiet (1988) who introduced the concept of 'minimum sweep', i.e. the minimum sweep that still avoids generating a singularity (a logarithmic singularity in his particular case). We will reanalyse this situation because of a minor error in (or, more precisely, restriction in the use of) one of Amiet's results.

We start with the case of a non-translating propeller (or, alternatively, a helicopter rotor). The Mach number component of the leading edge, normal to itself, in the direction of an observer at θ has a peak value of $M_{obs} = zM_t \cos\Lambda \sin\theta$ at $\phi = -\frac{1}{2}\pi + \Lambda$ and thus is maximum for an observer at $\theta = \frac{1}{2}\pi$, i.e. for an observer in the plane of the rotor – as would be expected intuitively. If, then, we choose the local sweep angle $\Lambda(z)$ so that

$$zM_t \cos\Lambda = 1 \tag{41}$$

we have $M_{obs} \leqslant 1$ everywhere, with the equality being satisfied only at $\theta = \frac{1}{2}\pi$. The variation in the azimuthal sweep angle μ (see figure 2) along the blade then satisfies, from (22) and (23),

$$\frac{\mathrm{d}\mu}{\mathrm{d}z} = \frac{\tan\Lambda}{z} \tag{42}$$

so that, using (41), we obtain $\mathrm{d}\mu/\mathrm{d}z = (z^2M_t^2 - 1)^{1/2}/z$ or, on integrating,

$$\mu = (z^2M_t^2 - 1)^{1/2} - \tan^{-1}(z^2M_t^2 - 1)^{1/2}, \tag{43}$$

in agreement with Amiet's result for a non-translating propeller.

We now turn to the case of a translating propeller. For a point on the leading edge

at radial station z the Mach number in the direction of an observer at θ in the (x, y)-plane is $M_{obs} = -zM_t \sin\phi \sin\theta + M_x \cos\theta$. Our intention is to construct the blade leading edge so that the maximum value of M_{obs}, when the blade is moving normal to itself, is unity. We need, therefore, to maximize M_{obs} subject to the constraints that the maximum value of M_{obs} must be unity ($-zM_t \sin\phi \sin\theta + M_x \cos\theta = 1$), and that the blade leading edge moves normal to itself; this second constraint is given, formally, by (29). Using the method of Lagrange multipliers we construct the function

$$L(\theta, \phi) = -zM_t \sin\phi \sin\theta + M_x \cos\theta + \lambda_1(-zM_t \sin\phi \sin\theta + M_x \cos\theta - 1) + \lambda_2[-(M_x/zM_t)\tan\Lambda \cos\theta + \cos\phi \sin\theta + \sin\phi \tan\Lambda \sin\theta], \quad (44)$$

where λ_1 and λ_2 are the multipliers, and find, after the usual process and a little manipulation, that the maximum value of M_{obs}, satisfying the constraints, occurs when

$$\theta = \cos^{-1}(M_x/M_r^2) \quad (45)$$

and the blade leading-edge angle Λ is given by

$$\tan\Lambda = (zM_t/M_r)(M_r^2 - 1)^{1/2}. \quad (46)$$

The results differs from that of Amiet who obtained $\tan\Lambda = (z^2M_t^2/\beta^2 - 1)^{1/2}$, where $\beta = (1 - M_x^2)^{1/2}$. The minor error has been acknowledged by Amiet (1994, personal communication) who pointed out, however, that his solution would be valid for an unconventional swept blade design in which the blade leading edge is constrained to move in a plane normal to the x-axis – a configuration which Amiet describes as non-optimal. Amiet's solution can easily be obtained by keeping $dx/dz = 0$ in (27)–(30) which, along with (31), lead to $zM_t \sin\theta \cos\Lambda/(1 - M_x \cos\theta) \leqslant 1$. The peak value of the left-hand side is $zM_t \cos\Lambda/\beta$ when $\cos\theta = M_x$. We thus ensure that the blade leading edge is, at most, transonic by setting $\cos\Lambda = \beta/(zM_t)$, or, on using (42) and integrating, $\mu = (z^2M_t^2/\beta^2 - 1)^{1/2} - \tan^{-1}(z^2M_t^2/\beta^2 - 1)^{1/2}$ in agreement with Amiet's result.

The blade leading edge on the conventional – or optimal – swept blade design can be determined from (42) and (46); by integrating and using Gradshteyn & Ryzhik (1965, §3.152.5 and §3.153.4) we obtain, after a little manipulation,

$$\mu = \frac{M_r}{zM_t}(M_r^2 - 1)^{1/2} - E\left[\cos^{-1}\left(\frac{\beta}{zM_t}\right), M_x\right], \quad (47)$$

where $E(\psi, k) = \int_0^{\psi}(1 - k^2 \sin^2\alpha)^{1/2}\, d\alpha$ is the elliptic integral of the second kind.

In figure 4 we show the planform of two blades with minimum leading-edge local sweep angle Λ for (*a*) a propeller with tip rotational Mach number $M_t = 0.8$ and forward Mach number $M_x = 0.8$, and (*b*) a propeller with tip rotational Mach number $M_t = 1.2$ and forward Mach number $M_x = 0$. These Mach numbers are typical for advanced propellers operating at 'cruise' and 'take-off' conditions respectively. Note that the leading-edge sweep parameter s_L can be obtained from (47) as $s_L = \mu M_r/M_t$.

4.2. *The tip contribution*

We suppose now that the blades have been swept sufficiently to ensure that the Mach number component normal to the leading edge is everywhere subsonic. The leading-order contributions (18) from the stationary phase points (or, following Chako 1965, interior critical points) are, therefore, no longer present. The next-order terms can be calculated either by considering (2) as a one-dimensional integral and using asymptotic properties of the Bessel function with large argument, large order and argument greater than order (this approach was taken by Crighton & Parry 1991), or by following

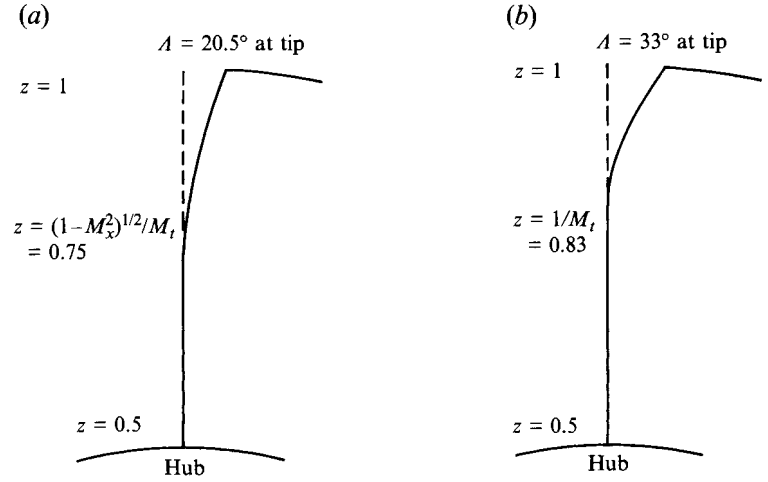

FIGURE 4. Blade planforms with 'critical' leading-edge designs: (*a*) $M_x = 0.8$, $M_t = 0.8$, $\theta = \cos^{-1}M_x = 37°$, blade shape calculated from (47); (*b*) $M_x = 0$, $M_t = 1.2$, $\theta = 90°$, blade shape calculated from (43).

Chako's double integral method in which the next-order contributions come from boundary critical points. Here, for consistency with our approach in §2 (and, further, with our calculations below in §5), we use Chako's method.

Boundary critical points are those points on the boundary of the domain of integration at which the tangential derivative of $f(z, t)$ vanishes. In our case the domain is an annular region described by the radial coordinate z and the angle t (in fact t is related, quite simply, to the azimuthal angle ϕ by $t = -\phi$). The tangential derivative of f vanishes, therefore, when $\partial f/\partial t = 0$ so that boundary critical points arise when $\partial f/\partial t = 0$ and $z = 1$ or $z = z_0$. Here we neglect the contribution from the hub since it usually moves subsonically thus giving only an exponentially small contribution (see Parry & Crighton 1989). For the unusual case of a propeller with a high hub/tip ratio and supersonic tip speed sufficiently high that the hub is also moving supersonically, an approach identical to that given below can be used to calculate the hub contribution.

From (12) the boundary critical points arise when $z = 1$ and $\sin t = z^*$ producing two solutions $(\hat{z}, \hat{t}_\pm)$ where

$$\hat{z} = 1, \quad \hat{t}_\pm = \begin{cases} \sin^{-1} z^* \\ \pi - \sin^{-1} z^*. \end{cases} \tag{48}$$

By expanding $S(z)$ and $f(z, t)$ in Taylor series about these points we find that the two contributions $P_m^\pm$ from the tip to (9) are, to leading order, given by the double integrals $(\pm)$

$$P_m^\pm \sim \frac{S_L(1)\,\mathrm{e}^{\mathrm{i}mBf_{0,0}}}{2\pi \mathrm{i}^{mB}} \int_{-\infty}^{1} \mathrm{e}^{\mathrm{i}mB(z-1)f_{1,0}}\,\mathrm{d}z \int_{-\infty}^{\infty} \mathrm{e}^{\mathrm{i}mB(t-\hat{t}_\pm)^2 f_{0,2}/2}\,\mathrm{d}t, \tag{49}$$

where the partial derivatives $f_{j,k}$ here are evaluated at $z = \tilde{z} = 1$, $t = \hat{t}_\pm$. The integrals are easily calculated as

$$P_m^\pm \sim \frac{S_L(1)\exp\left[\mathrm{i}mBf_{0,0} + \mathrm{i}\tfrac{1}{4}\pi\,\mathrm{sgn}\,(mB)\,\mathrm{sgn}\,(f_{0,2})\right]}{\mathrm{i}^{mB+1}(2\pi)^{1/2}\,mB|mB|^{1/2} f_{1,0}|f_{0,2}|^{1/2}}. \tag{50}$$

Adding the two solution (50) for $t = \hat{t}_+$ and $t = \hat{t}_-$, and substituting for our original variables we obtain

$$P_m \sim \frac{S_L(1)\,\mathrm{e}^{-\mathrm{i}mB\psi_s(1)-\mathrm{i}\pi/2}}{(2\pi)^{1/2}mB|mB|^{1/2}(\tan\hat{\phi})^{1/2}}\left\{\frac{\exp[\mathrm{i}mB(\tan\hat{\phi}-\hat{\phi})-\mathrm{i}\frac{1}{4}\pi\,\mathrm{sgn}(mB)]}{\tan\hat{\phi}-\psi_s'(1)}\right.$$
$$\left.-\frac{\exp[-\mathrm{i}mB(\tan\hat{\phi}-\hat{\phi})+\mathrm{i}\frac{1}{4}\pi\,\mathrm{sgn}(mB)]}{\tan\hat{\phi}+\psi_s'(1)}\right\}, \quad (51)$$

where, for comparison with the alternative Bessel function approach, we have replaced $\hat{t}_+$ by $\hat{\phi} = \frac{1}{2}\pi - \hat{t}_+$ – given as β in Crighton & Parry (1991).

Our present calculation has assumed that the source strength $S(z)$ is non-zero at the blade tips. In general, however, this is not necessarily true; e.g. rounded blade tips would produce a thickness source strength that dropped to zero at $z = 1$ and a spanwise blade loading distribution similar to the elliptical distributions commonly found on wings would also result in a source strength tending to zero at the tips. The case in which $S(z)$ drops to zero at $z = 1$ can, however, also be treated by the present approach. We put, simply,

$$S(z) \sim \eta(1-z)^{\sigma} \quad \text{as} \quad z \to 1 \quad (52)$$

so that the leading-order term is $O[S(1)\,|mB|^{-3/2-\sigma}]$ instead of $O[S(1)\,|mB|^{-3/2}]$ as in (51). Here the precise dependence on mB is obtained by filling in the dependence of $S(z)$ on mB, where $S(z)$ – taken to be either $S_L(z)$ or $S_T(z)$ – includes both source strength and non-compactness effects.

4.3. *Singularities radiated from the tip*

The question now arises as to whether singularities can still be radiated from a supersonic propeller with a completely subsonic leading edge. In this situation – where there is no 'swept-blade' Mach radius – the dominant term clearly arises from the tip contribution. We calculate the precise order of the leading term following the approach in §3. Then, on combining source strength, chordwise non-compactness and tip edge effects we find that, for thickness noise, the leading term is of the form

$$P_m \sim |mB|^{-\nu_L-1/2}\{\mathrm{sgn}(mB)\cos[(\nu_L+1)\tfrac{1}{2}\pi \pm \tfrac{1}{4}\pi] - \mathrm{i}\sin[(\nu_L+1)\tfrac{1}{2}\pi \pm \tfrac{1}{4}\pi]\}, \quad (53)$$

where we have given only the leading-edge contribution at the tip; a similar term arises from the trailing edge at the tip with ν_L replaced by ν_T, where ν_L and ν_T are the leading- and trailing-edge source gradient orders defined in (33). In (53) the additive constants of $\pm\frac{1}{4}\pi$ in the cosine and sine terms arise directly from the two phase terms in (51); the upper and lower signs represent the contributions from $t = \hat{t}_+$ and $t = \hat{t}_-$ respectively.

We can now consider three distinct cases, corresponding to different values of the source gradient order ν_L, which differ, somewhat, from the three cases examined previously in §3 for radiation from the 'swept-blade' Mach radius. All of these cases can include 'blunt' leading edges (with differing degrees of bluntness), although the last case to be considered also includes sharp edges. First we specify that the source gradient order satisfies $0 < \nu_L < \frac{1}{2}$ and thus obtain a time-domain solution containing weak algebraic singularities of the form $\mathrm{sgn}(t)\,|t|^{-(1/2-\nu_L)}$ and $|t|^{-(1/2-\nu_L)}$ from the cosine and sine terms in (53) respectively. Next we consider a blade tip with a parabolic leading edge so that the source gradient order $\nu_L = \frac{1}{2}$. Here we treat the upper and lower signs in (53) separately. The contribution from $t = \hat{t}_+$ comes solely from the cosine term and produces an acoustic waveform with pressure discontinuities – or shocks – of the form $\mathrm{sgn}(t)$. The contribution from $t = \hat{t}_-$ comes solely from the sine term and produces a real-time waveform containing $\ln|t|$ logarithmic singularities. This solution

is particularly interesting as the two separate solutions are radiated at different azimuthal positions; we will discuss this point further below. Finally, we consider leading edges for which the source gradient order $\nu_L > \frac{1}{2}$; this case thus includes wedge-shaped and cusp-shaped leading edges. Here, by inverting (53), we obtain solutions of the form $\operatorname{sgn}(t)|t|^{\nu_L-1/2}$ and $|t|^{\nu_L-1/2}$ thus producing a smooth waveform.

The sharp-edged airfoils examined by Amiet (1988) will, then, clearly produce non-singular solutions when the blades are swept so that the leading edge is everywhere subsonic. However, it is very important to note that supersonic airfoils with blunt leading edges will continue to radiate singularities, or discontinuities, even when the leading edge is effectively subsonic, the singularities/discontinuities being radiated from the blade tip. The radiation of inverse square-root singularities from blade tips with a blunt leading edge has been discussed previously by Tam (1983). However, Tam was concerned solely with straight blades and transonic tips. It was, therefore, previously unclear whether or not the singularities were associated specifically with a tip effect or a transonic effect. In addition, combining the results of both Amiet (1988) and Tam (1983), it was unclear whether sweeping the blade would remove the singularities from the sound field. The description above shows that singularities can emanate from either a Mach radius or the tip. Clearly any singularities associated specifically with a Mach radius will be removed completely by sweeping the blade sufficiently. The singularities radiated from the tip, however, are not a transonic phenomenon but represent a supersonic edge effect (where *edge* means the leading or trailing edge at the tip) which cannot be removed by sweeping the blade; they can only be removed either by providing a sharp leading edge (actually, this is too stringent a specification; we require, for preciseness, merely that the source gradient order $\nu_L > \frac{1}{2}$) at the tip, or by rounding the blade at the tip, as described by (52), so that

$$\sigma + \nu_L > \tfrac{1}{2}. \tag{54}$$

A discussion similar to that given above applies to blade loading noise. Here, combining all effects, the leading-order term is of the form

$$P_m \sim |mB|^{-\nu_L-3/2}\{\cos[(\nu_L+1)\tfrac{1}{2}\pi \pm \tfrac{1}{4}\pi] - \mathrm{i}\operatorname{sgn}(mB)\sin[(\nu_L+1)\tfrac{1}{2}\pi \pm \tfrac{1}{4}\pi]\}, \tag{55}$$

where, as before, we have given only the leading-edge contribution and the $\pm\frac{1}{4}\pi$ terms are associated with $t = \hat{t}_+$ and $t = \hat{t}_-$ respectively. As for thickness noise we consider three cases corresponding to different values of the source gradient order ν_L. First, for $-1 < \nu_L < -\frac{1}{2}$, we obtain weakly singular solutions of the form $p(t) \sim |t|^{-(-\nu_L-1/2)}$ and $p(t) \sim \operatorname{sgn}(t)|t|^{-(-\nu_L-1/2)}$ from the cosine and sine terms in (55) respectively. Secondly, for $\nu_L = -\frac{1}{2}$ we obtain two distinct solutions: a pressure discontinuity, or shock, $p(t) \sim \operatorname{sgn}(t)$ from $t = \hat{t}_+$; and a logarithmic singularity $p(t) \sim \ln|t|$ from $t = \hat{t}_-$. Finally, when the source gradient order $\nu_L > -\frac{1}{2}$ we obtain smooth solutions of the form $p(t) \sim |t|^{\nu_L+1/2}$ and $p(t) \sim \operatorname{sgn}(t)|t|^{\nu_L+1/2}$.

In order to remove singularities from the loading noise sound field, therefore, we require, in addition to a completely subsonic leading edge, that the source gradient order for the leading-edge loading at the tip satisfies $\nu_L > -\frac{1}{2}$, or that the loading drops to zero at the tip with (54) being satisfied.

5. The Mach plane

The discussion so far has informed us of the radial stations from which singularities are radiated – namely the Mach radius or the tip – and the form of the singularities. However, even without knowing the swept-blade geometry, we still have sufficient

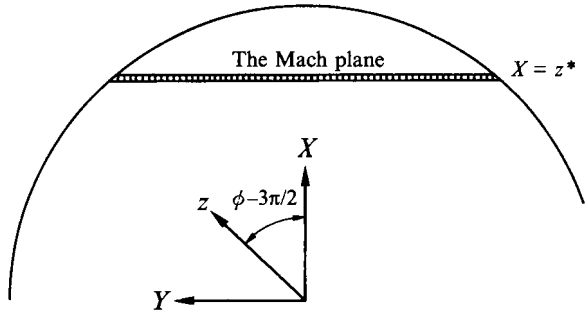

FIGURE 5. The Mach plane.

information to calculate in more detail the positions in the disk plane at which singularities are generated.

5.1. *Mach radii*

Any radial station $z = \tilde{z}$ qualifying as a Mach radius (as we commented earlier, a swept propeller can have more than one Mach radius) satisfies (13) so that

$$\tilde{z}\sin(-\phi) = z^*. \tag{56}$$

This result tells us that, whatever the geometry of the blade, singularities – if they exist – are generated when the swept-blade Mach radii cut through a plane which lies a distance z^* from the centre of the propeller disk and is parallel to the plane containing the propeller flight axis and the observer. We will call this plane the 'Mach plane' (see figure 5 which, for ease of interpretation, has been rotated by π). Since ϕ is related to the integration parameter t by $\phi = -t$ we also have, from (13) and (23), that

$$\tilde{z}\cos\phi = z^* \tan\Lambda/(1 - M_x\cos\theta). \tag{57}$$

Then, for $\Lambda > 0$ (representing backward swept propeller blades) the solutions lies in $-\frac{1}{2}\pi < \phi < 0$, and for $\Lambda < 0$ (forward swept blades) in $-\pi < \phi < -\frac{1}{2}\pi$. For an observer on the other side of the propeller it is easily seen, by rotating the x, y axes through 180°, that the singularities are generated a distance z^* above the (x, y)-plane where, of course, the blades are moving towards the observer.

5.2. *Supersonic tips*

Any singularities radiated from the tips are generated, from (56), when

$$\sin\phi = -z^*, \quad z = 1. \tag{58}$$

More specifically this result shows, again, that the singularities are radiated when the blade tips cross the Mach plane. At this point the speed of the blade tip towards an observer at θ is $M_{obs} = -M_t\sin\phi\sin\theta + M_x\cos\theta$ which, from (1), becomes $M_{obs} = 1$, i.e. the singularities are generated when the blade tip speed is sonic in the direction of the observer – whatever the details of blade sweep at the tip.

For the particular cases of thickness noise radiated from a parabolic leading edge, and loading noise radiated from a leading edge sustaining an inverse square-root singularity (in the loading), we found in §4 that the contributions from $t = \hat{t}_+$ and $t = \hat{t}_-$ produced different singularities: a pressure discontinuity – or shock – is radiated when the leading edge at the blade tip cuts the Mach plane and $t = \hat{t}_+$, or $\phi = -\sin^{-1} z^*$, i.e. the blade is on its 'up stroke'; a logarithmic singularity is radiated when the leading edge at the blade tip cuts the Mach plane and $t = \hat{t}_-$, or $\phi = -\pi + \sin^{-1} z^*$, i.e. the blade is on its 'down stroke'.

6. More singular solutions

6.1. *The focusing Mach radius*

We now consider whether it is possible for a swept propeller to radiate discontinuities that are more singular than those radiated by a straight-bladed propeller. To do this we return to the double-integral formulation (9) and consider the work of Chako (1965). Chako showed that the leading contribution of $O(1/mB)$ from 'interior critical points' (stationary phase points) could be superseded by a contribution from an interior critical point which is also a 'caustic' or 'focus', i.e. when the denominator in (18) vanishes.

We proceed, as in §2 to expand $f(z,t)$ in a Taylor series about a Mach point $z=\tilde{z}$, $t=\tilde{t}$. Including third-order terms we find, after using the simple transformation (17), that

$$\begin{aligned} f(z,t) = f_{0,0} &+ \frac{1}{2}\left(f_{2,0} - \frac{f_{1,1}^2}{f_{0,2}}\right) Z^2 + \tfrac{1}{2} f_{0,2}\, T^2 \\ &+ \frac{1}{6}\left(f_{3,0} - 3\frac{f_{2,1} f_{1,1}}{f_{0,2}} + 3\frac{f_{1,2} f_{1,1}^2}{f_{0,2}^2} - \frac{f_{0,3} f_{1,1}^3}{f_{0,2}^3}\right) Z^3 \\ &+ \frac{1}{2}\left(f_{2,1} - 2\frac{f_{1,2} f_{1,1}}{f_{0,2}} + \frac{f_{0,3} f_{1,1}^2}{f_{0,2}^2}\right) Z^2 T \\ &+ \frac{1}{2}\left(f_{1,2} - \frac{f_{0,3} f_{1,1}}{f_{0,2}}\right) Z T^2 + \tfrac{1}{6} f_{0,3}\, T^3 \\ &+ \text{higher order terms.} \end{aligned} \tag{59}$$

If we now suppose that (14) is not just satisfied at the discrete points $z=\tilde{z}$ but is satisfied analytically close to† $z=\tilde{z}$ then we can differentiate (14) to obtain

$$\psi_s'(z)\,\psi_s''(z) - 1/z^3 = 0. \tag{60}$$

Then, at $z=\tilde{z}$ where $\partial f/\partial z = \partial f/\partial t = 0$, we can combine (12) and (60) resulting in $f_{2,0} f_{0,2} - f_{1,1}^2 = 0$ so that the coefficient of Z^2 in (59) disappears. We define $c_{i,j}$ to be the coefficient of the term in $Z^i T^j$, i.e.

$$\left.\begin{aligned} &c_{0,0} = f_{0,0}, \quad c_{0,2} = f_{0,2}, \quad c_{3,0} = f_{3,0} - 3\frac{f_{2,1} f_{1,1}}{f_{0,2}} + 3\frac{f_{1,2} f_{1,1}^2}{f_{0,2}^2} - \frac{f_{0,3} f_{1,1}^3}{f_{0,2}^3}, \\ &c_{2,1} = f_{2,1} - 2\frac{f_{1,2} f_{1,1}}{f_{0,2}} + \frac{f_{0,3} f_{1,1}^2}{f_{0,2}^2}, \quad c_{1,2} = f_{1,2} - \frac{f_{0,3} f_{1,1}}{f_{0,2}}, \quad c_{0,3} = f_{0,3}, \end{aligned}\right\} \tag{61}$$

and introduce the additional transformation

$$\zeta = Z + \frac{c_{2,1}}{c_{3,0}} T, \quad \tau = T, \tag{62}$$

for which the Jacobian is again unity, so that, after a little manipulation,

$$\begin{aligned} f(z,t) = c_{0,0} + \tfrac{1}{2} c_{0,2}\, \tau^2 &\left[1 + \frac{(c_{1,2} c_{3,0} - c_{2,1}^2)}{c_{0,2} c_{3,0}} \zeta + \frac{(c_{0,3} c_{3,0}^2 - 3 c_{2,1} c_{1,2} c_{3,0} + 2 c_{2,1}^3)}{3 c_{0,2} c_{3,0}^2} \tau\right] \\ &+ \tfrac{1}{6} c_{3,0}\, \zeta^3 + \text{higher order terms.} \end{aligned} \tag{63}$$

† Here we mean close to $z=\tilde{z}$, and only close to $z=\tilde{z}$; if, in fact, (14) is satisfied analytically over a finite interval then an even more singular result follows – see below.

The integral (9) is then, to leading order, given by

$$P_m \sim \frac{S(\tilde{z})\mathrm{e}^{\mathrm{i}mBc_{0,0}}}{2\pi \mathrm{i}^{mB}} \int_{-\infty}^{\infty} \mathrm{e}^{\mathrm{i}mBc_{0,2}\tau^2/2}\mathrm{d}\tau \int_{-\infty}^{\infty} \mathrm{e}^{\mathrm{i}mBc_{3,0}\zeta^3/6}\,\mathrm{d}\zeta$$

$$= \frac{(-\frac{2}{3})!}{\pi^{1/2}6^{1/6}|c_{0,2}|^{1/2}|c_{3,0}|^{1/3}} \frac{S(\tilde{z})\,\mathrm{e}^{\mathrm{i}mB(c_{0,0}-\pi/2)+\mathrm{i}\,\mathrm{sgn}(mB)\,\mathrm{sgn}(c_{0,2})\pi/4}}{|mB|^{5/6}}. \tag{64}$$

This result is $O(|mB|^{-5/6})$ and shows clearly that the field radiated from a caustic will be more singular than that radiated from a supersonic straight-bladed propeller. Specifically, using the results from §3, we find that, for thickness noise, the harmonic components of the radiated sound field contain terms of the form

$$P_m \sim |mB|^{1/6-\nu_L}, \quad P_m \sim |mB|^{1/6-\nu_L}\,\mathrm{sgn}(mB); \tag{65}$$

there are thus four interesting types of blade shape to consider, corresponding to different values of the source gradient order ν_L. First, for $0 < \nu_L < \frac{1}{6}$ (representing a very blunt airfoil), strong algebraic singularities of the form $|t|^{-1-(1/6-\nu_L)}$ and $|t|^{-1-(1/6-\nu_L)}\,\mathrm{sgn}(t)$ are radiated. Secondly, for $\frac{1}{6} < \nu_L < \frac{7}{6}$ (representing blunt airfoils for $\frac{1}{6} < \nu_L < 1$, wedge-shaped airfoils for $\nu_L = 1$ and weakly cusped airfoils for $1 < \nu_L < \frac{7}{6}$), weak algebraic singularities of the form $|t|^{-1+(\nu_L-1/6)}$ and $|t|^{-1+(\nu_L-1/6)}\,\mathrm{sgn}(t)$ are generated. Thirdly, for the specific case $\nu_L = \frac{7}{6}$, logarithmic singularities and pressure discontinuities are radiated. Finally, for $\nu_L > \frac{7}{6}$ (cusped airfoils), there are no singularities and we obtain a smooth waveform. Similar results follow for steady loading noise with ν_L, in each case, reduced by 1. For non-singular radiation the leading edge must thus be lightly loaded with $\nu_L > \frac{1}{6}$. These results are important in showing precisely how, at a caustic (or focus) condition, the radiation from a swept airfoil is more singular than that from a straight-bladed propeller.

We need to understand, though, the circumstances under which a caustic can arise. Since (14) is satisfied analytically – even on just a vanishingly small region close to $z = \tilde{z}$ – we can integrate to find, on using (22), that a caustic will arise for radiation in direction θ when the local blade leading-edge shape is given by

$$\mu = (1 - M_x\cos\theta)\left\{\left[\frac{z^2M_t^2\sin^2\theta}{(1-M_x\cos\theta)^2} - 1\right]^{1/2} - \tan^{-1}\left[\frac{z^2M_t^2\sin^2\theta}{(1-M_x\cos\theta)^2} - 1\right]^{1/2}\right\}. \tag{66}$$

Comparing this with (43) we see that it represents the generalization of the 'minimum sweep' result for arbitrary radiation angle θ and for $M_x \neq 0$. If then, for any angle θ, the blade shape over an element, centred on the swept-blade Mach radius, is given by (66), then the radiation in direction θ is given by (64) and hence is of lower order in $1/mB$ – and therefore more singular – than that given by the standard result (18). Physically, this result means that each point of the blade element radiates singularities as it cuts the Mach plane, with the radiation being focused on the observer at θ. Referring back to the discussion in §4 for a non-translating propeller we see that, for an observer at $\theta = \frac{1}{2}\pi$ the 'minimum sweep' geometry, whilst reducing the radiation to observers at all other angles, can result in the radiation of an enhanced singularity (depending on the leading-edge shape or loading) in direction $\theta = \frac{1}{2}\pi$. The general solution (66) shows that variations in leading-edge geometry can lead to the radiation of these singularities in different directions – for both non-translating and translating propellers. Note, however, that the formal *minimum sweep* design for a translating

propeller, given by (47), does not lead to an enhanced singularity since, from (45), the singularities from each radius radiate in different directions instead of accumulating in one fixed direction.

It is important that we emphasize, once again, that the caustic arises when the blade leading-edge shape is only given locally by (66); when (66) holds over a finite interval the effect is even more significant.

6.2. *The focusing Mach plane*

We now consider the situation in which (14) is satisfied over a finite interval, taken to be from the straight-blade Mach radius $z = z^*$ to the tip $z = 1$. We have already determined that singularities are radiated when discrete Mach radii cut through the Mach plane; when these Mach radii stretch continuously from $z = z^*$ to $z = 1$, however, singularities are radiated when every part of a blade cuts through the Mach plane (on the up stroke). Accordingly, stationary phase points lie along the intersection of the Mach plane with half of the propeller disk. It is appropriate, therefore, to change to Cartesian coordinates (X, Y) as shown in figure 5. The result is, of course, a continuous distribution of stationary points along $X = z^*$, $0 < Y < (1-z^{*2})^{1/2}$. We note that the analysis applies, particularly, to the *minimum sweep* design for a non-translating propeller, derived by Amiet and given here by (43). After some manipulation we find (see the Appendix), that the radiation is, to leading order, given by

$$P_m \sim \left(\frac{z^*}{2\pi|mB|}\right)^{1/2} \mathrm{e}^{-\mathrm{i}\pi/4} \int_{z^*}^{1} \frac{S_L(z)}{(z^2-z^{*2})^{1/4}}\, z. \tag{67}$$

Radiation from the trailing edge is obtained by replacing $S_L(z)$ with $S_T(z)$.

This result is $O(|mB|^{-1/2})$ and thus represents radiation even more singular than that from a caustic. Specifically, we examine the effects of five types of leading-edge shape, corresponding to different values of the source gradient order ν_L, on thickness noise. First, for $0 < \nu_L < \frac{1}{2}$ (representing blunt leading edges) strong algebraic singularities, $|t|^{-1-(1/2-\nu_L)}$ and $|t|^{-1-(1/2-\nu_L)}\,\mathrm{sgn}\,(t)$, will be radiated. Secondly, for $\nu_L = \frac{1}{2}$ (parabolic leading edge) singular pulses, $\delta(t)$, and pole singularities of order one, $1/t$, will be radiated. Thirdly, for $\frac{1}{2} < \nu_L < \frac{3}{2}$ (representing blunt leading edges for $\frac{1}{2} < \nu_L < 1$, wedge-shaped leading edges for $\nu_L = 1$, and cusped leading edges for $\nu_L > 1$) weak algebraic singularities, $|t|^{-1+(\nu_L-1/2)}$ and $|t|^{-1+(\nu_L-1/2)}\,\mathrm{sgn}\,(t)$, will be radiated. Fourthly, for $\nu_L = \frac{3}{2}$ (a specific cusp-shaped leading edge) logarithmic singularities and pressure discontinuities – or shocks – are radiated. Finally, when $\nu_L > \frac{3}{2}$ the radiation is of the form $|t|^{\nu_L-3/2}$ or $|t|^{\nu_L-3/2}\,\mathrm{sgn}\,(t)$ and, therefore, produces a smooth waveform.

Similar results follow for steady loading noise where the corresponding value of the source gradient order ν_L is reduced by 1 in each case. Non-singular radiation occurs when the leading edge is lightly loaded with $\nu_L > \frac{1}{2}$.

7. Results

7.1. *Leading-edge geometry and asymptotic solutions*

In this section we will present, and discuss, results obtained for supersonic, transonic and subsonic leading edges. We consider two different flight conditions: a 'cruise' condition with $M_x = 0.8$, $M_t = 0.8$ and the peak radiation angle $\theta = \cos^{-1} M_x = 36.9°$; and a possible 'take-off' condition with $M_x = 0$, $M_t = 1.2$ and the peak radiation angle $\theta = 90°$ (i.e. peak radiation is in the plane of the propeller). We also calculate results for thickness noise generated by blunt and sharp leading-edge shapes; in both cases the

trailing edges are designed to be sharper than the leading edges so that the radiation from the trailing edges can be neglected as $mB \to \infty$. Loading noise results are not given here but, we emphasize, can be obtained in precisely the same manner; all that is required is a knowledge of the chordwise loading distribution.

In the results to follow, the thickness/chord ratio for the airfoil with the blunt leading edge is given by

$$h/c = (b/c)(1.485X^{1/2} - 0.63X - 1.758X^2 + 1.422X^3 - 0.519X^4) \tag{68}$$

and is the same as that used by Tam (1983). The airfoil thus has a parabolic leading edge (the source gradient order $\nu_L = \frac{1}{2}$), since $h/c \sim 1.485X^{1/2}b/c$ as $X \to 0$, and a wedge-shaped trailing edge (the source gradient order $\nu_T = 1$), since $h/c \sim 1.2135(1-X)b/c$ as $X \to 1$. The airfoils with sharp leading edges are taken to have thickness/chord ratios given by

$$h/c = 3.375(b/c)X(1-X)^2. \tag{69}$$

The airfoils thus have wedge-shaped leading edges (the source gradient order $\nu_L = 1$), since $h/c \sim 3.375Xb/c$ as $X \to 0$, and cusp-shaped trailing edges (the source gradient order $\nu_T = 2$), since $h/c \sim 3.375(1-X)^2 b/c$ as $x \to 1$. We suppose, for simplicity, that the airfoil chord and maximum thickness are constant. The source strength $S(z)$ for thickness noise is thus independent of z. It is, however, most important to note that the asymptotic leading-edge source strength $S_L(z)$, and trailing-edge source strength $S_T(z)$, are not independent of z since the wavenumber k_x depends on the section relative Mach number M_r which, of course, increases with z.

We start with a straight leading edge, and of course a supersonically operating propeller, and gradually increase the sweep towards the 'critical' design, i.e. the leading edge is defined, for $z > z^*$, by

$$\mu = \lambda(1 - M_x \cos\theta)\left[\left(\frac{z^2}{z^{*2}} - 1\right)^{1/2} - \tan^{-1}\left(\frac{z^2}{z^{*2}} - 1\right)^{1/2}\right], \tag{70}$$

with $\mu = 0$ for $z \leqslant z^*$ and λ, a scale factor or sweep parameter, taking values between 0 and 1. When $\lambda = 0$ the blade is straight; when $\lambda = 1$ the blade sweep is identical to that in (66) and the design is therefore critical; when $0 < \lambda < 1$ the blade sweep, at each radial station, is simply a fraction λ of that on the critical design. For all such leading-edge shapes there is, from (14), a single Mach radius at $z = *$ producing, from (18), a leading-order contribution of

$$|P_m| \sim \frac{z^* S_L(z^*)}{|mB|(1-\lambda^2)^{1/2}}. \tag{71}$$

This result is, of course, invalid when $\lambda = 1$ since the design is then critical. We use, instead, the result (67) which, for arbitrary $S_L(z)$, can easily be integrated numerically. It is, however, interesting to note that for constant $S_L(z)$, the integral (67) can be evaluated as (see Gradshteyn & Ryzhik 1965, §3.183, p. 282)

$$P_m \sim \frac{z^* S_L(z^*)}{\pi^{1/2}|mB|^{1/2}} \left\{\mathrm{F}\left(\gamma, \frac{1}{\sqrt{2}}\right) - 2\mathrm{E}\left(\gamma, \frac{1}{\sqrt{2}}\right) + \frac{2(1-z^{*2})^{1/4}}{z^{*1/2}[z^* + (1-z^{*2})^{1/2}]}\right\}, \tag{72}$$

where F and E are elliptic integrals of the first and second kind respectively and

$$\gamma = \cos^{-1}\left(\frac{z^* - (1-z^{*2})^{1/2}}{z^* + (1-z^{*2})^{1/2}}\right). \tag{73}$$

Since the integral (67) is, perhaps, likely to be dominated by contributions from the weak singularity at $z = z^*$, (72) could be used as a first approximation to (67).

Increasing the value of λ beyond unity in (70) produces simply (71) again, with the square-root term replaced by $(\lambda^2-1)^{1/2}$, since the blade has, again, a single Mach radius at $z = z^*$. As an alternative we modify the leading-edge sweep so that a greater part of the blade span is swept and the leading edge is everywhere subsonic; we take, for $z > z^*/\lambda$,

$$\mu = (1-M_x\cos\theta)\left[\left(\frac{\lambda^2 z^2}{z^{*2}}-1\right)^{1/2}-\tan^{-1}\left(\frac{\lambda^2 z^2}{z^{*2}}-1\right)^{1/2}\right], \tag{74}$$

with $\mu = 0$ for $z \leqslant z^*/\lambda$ and λ taking values above unity. Here, then, the scale factor λ is applied to the radii instead of to the sweep. For this design the leading edge is, indeed, completely subsonic so that the dominant contribution to the sound field arises from the tip and, from (48) and (51), is given by

$$|P_m| \sim \frac{S_L(1)\,z^{*3/2}}{(2\pi)^{1/2}|mB|^{3/2}(1-z^{*2})^{1/4}}\left|\frac{\exp\left(2imB\{(1-z^{*2})^{1/2}/z^*-\tan^{-1}[(1-z^{*2})^{1/2}/z^*]\}\right)}{(1-z^{*2})^{1/2}-(\lambda^2-z^{*2})^{1/2}}\right.$$

$$\left.-\frac{\mathrm{i}}{(1-z^{*2})^{1/2}+(\lambda^2-z^{*2})^{1/2}}\right|. \tag{75}$$

7.2. *Comparison between numerical and asymptotic results*

Comparisons between full numerical calculations and asymptotic approximations are shown in figures 6–9. To help in understanding the figures we recall that λ represents a blade-sweep scale factor relative to that on a critical design with the sweep defined by (70) for $0 < \lambda \leqslant 1$ and (74) for $\lambda > 1$. The numerical results are obtained by numerical integration of (2) with the source strength function $S(z)$ given by the second expression in (5) and the integrand modified by the multiplying factor (32) – the chordwise non-compactness factor – in which the shape function $F(X)$ is given by (68) or (69) for blunt or sharp leading edges respectively. The asymptotic results are given by (71) for $\lambda < 1$, (67) for $\lambda = 1$ and (75) for $\lambda > 1$. In the figures the solid lines represent the full numerical solution, the dashed lines represent the asymptotic solutions for supersonic ($0 < \lambda < 1$) and subsonic ($\lambda > 1$) leading edges, and the black dot represents the asymptotic solution for a transonic leading edge ($\lambda = 1$). For each condition results are given for $mB = 20$, 30, 50 and 100.

Figure 6 shows the results for blunt leading-edge airfoil sections operating at the 'cruise' condition. For low values of mB the numerical solution remains roughly constant, as the blade sweep is increased, until the 'critical' condition is reached; further increases in sweep produce substantial reductions in level. For higher values of mB, however, the solution increases initially, reaching a peak value at $\lambda = 1$, before the levels reduce for highly swept blades. Clearly, the critical design ($\lambda = 1$) generates levels that are 5–10 dB higher, in the direction of peak radiation, than a straight-bladed design. Indeed, the effect of the critical design is emphasized in the figure for $mB = 50$ and 100 where the noise levels can be seen to drop initially before increasing rapidly close to $\lambda = 1$ and then dropping as the sweep is increased further. The asymptotic results agree extremely well with the numerical calculations, the agreement becoming more marked for high values of mB. This is particularly true for $\lambda < 1$, and indeed for $\lambda = 1$, where the 'enhanced' effect of the critical condition on the numerical calculations only becomes clear as mB is increased.

Results for sharp leading-edge airfoil sections operating at 'cruise' conditions are

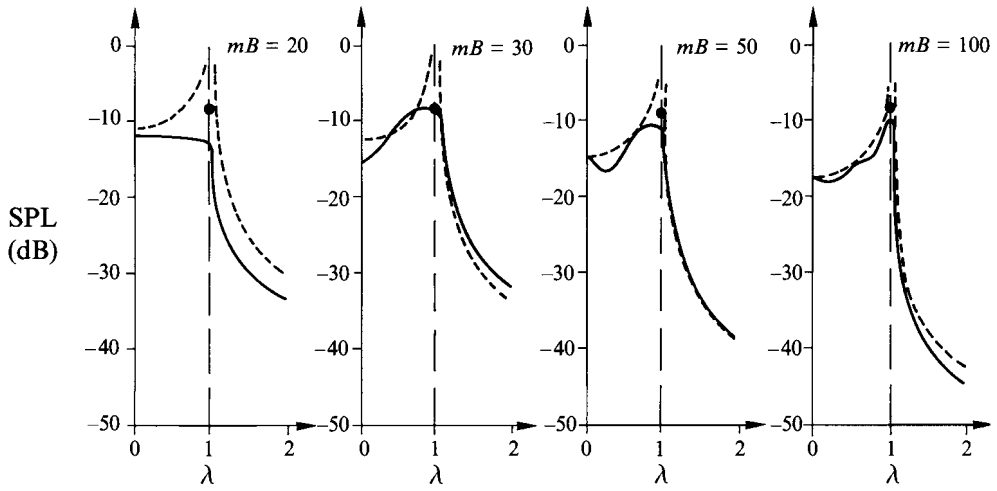

FIGURE 6. Comparison between numerical results and asymptotics for $0 \leqslant \lambda \leqslant 2$, parabolic leading edges, $M_x = 0.8$, $M_t = 0.8$, $\theta = 37°$; λ represents a blade-sweep scale factor relative to that on a critical design and is defined by (70) for $0 \leqslant \lambda \leqslant 1$ and (74) for $\lambda > 1$.

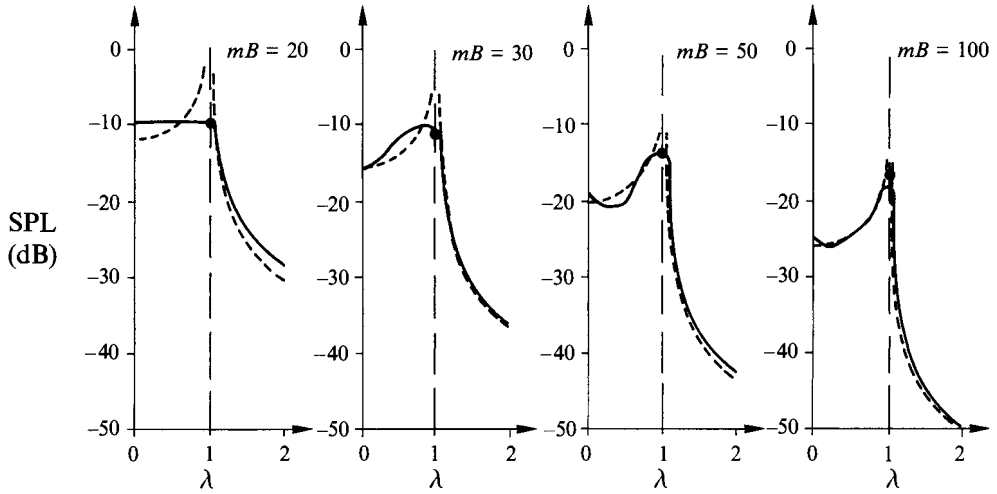

FIGURE 7. Comparison between numerical results and asymptotics for $0 \leqslant \lambda \leqslant 2$, wedge-shaped leading edges, $M_x = 0.8$, $M_t = 0.8$, $\theta = 37°$.

shown in figure 7. These results are almost identical to those in figure 6, except that noise levels for sharp leading edges are, typically, around 5–10 dB lower than those for blunt leading edges; this is, heuristically, in keeping with the results from §§3, 4 and 6 which showed that the radiation from blunt leading edges is always more singular than that from a sharp leading edge (typically, by a half power of time in the pressure waveform).

In figures 8 and 9 the results are given, for blunt and sharp leading-edge airfoil sections respectively, at 'take-off' conditions. As for 'cruise' conditions, the agreement between asymptotics and numerical calculations is very good and, indeed, increases at higher values of mB; the results for blunt leading edges are, typically 5 dB higher than those for sharp leading edges.

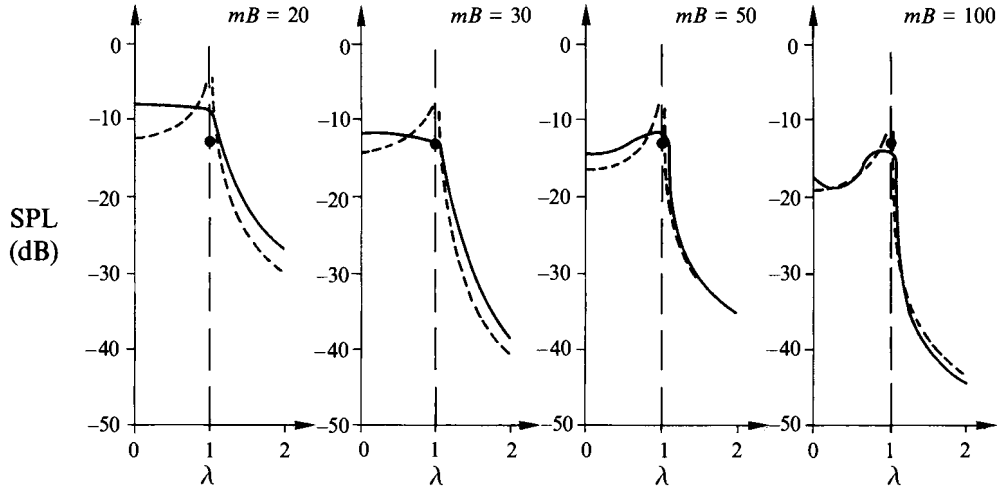

FIGURE 8. Comparison between numerical results and asymptotics for $0 \leqslant \lambda \leqslant 2$, parabolic leading edges, $M_x = 0$, $M_t = 1.2$, $\theta = 90°$.

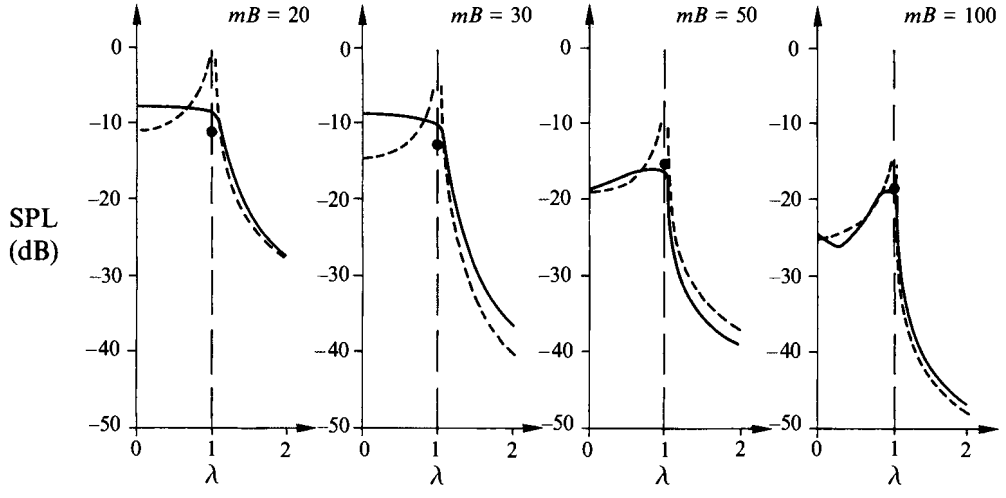

FIGURE 9. Comparison between numerical results and asymptotics for $0 \leqslant \lambda \leqslant 2$, wedge-shaped leading edges, $M_x = 0$, $M_t = 1.2$, $\theta = 90°$.

In some parts of figures 6–9 the agreement between numerical and asymptotic solutions for supersonic leading edges ($0 < \lambda < 1$) is not quite as good as we might expect, particularly near to $\lambda = 0$ which represents, of course, an unswept configuration. However, previous work (Crighton & Parry 1991) has shown that we can obtain much better agreement between numerics and asymptotics by adding higher-order terms to the solution, i.e. by adding the contributions from the tip to the leading-order Mach radius solution.

The asymptotic result for the 'critical' design ($\lambda = 1$) was calculated, in figures 6–9, by integrating (67) numerically. We remark in passing, however, that the use of the simplified result (70) seems to produce, at most, an error of 1.5 dB.

There is, however, one additional point to note in figures 8 and 9: although the levels should decay with mB [as $(mB)^{-1}$ for blunt leading edges and as $(mB)^{-3/2}$ for sharp leading edges] the results for $mB = 50$ are clearly higher than those for $mB = 30$ in the

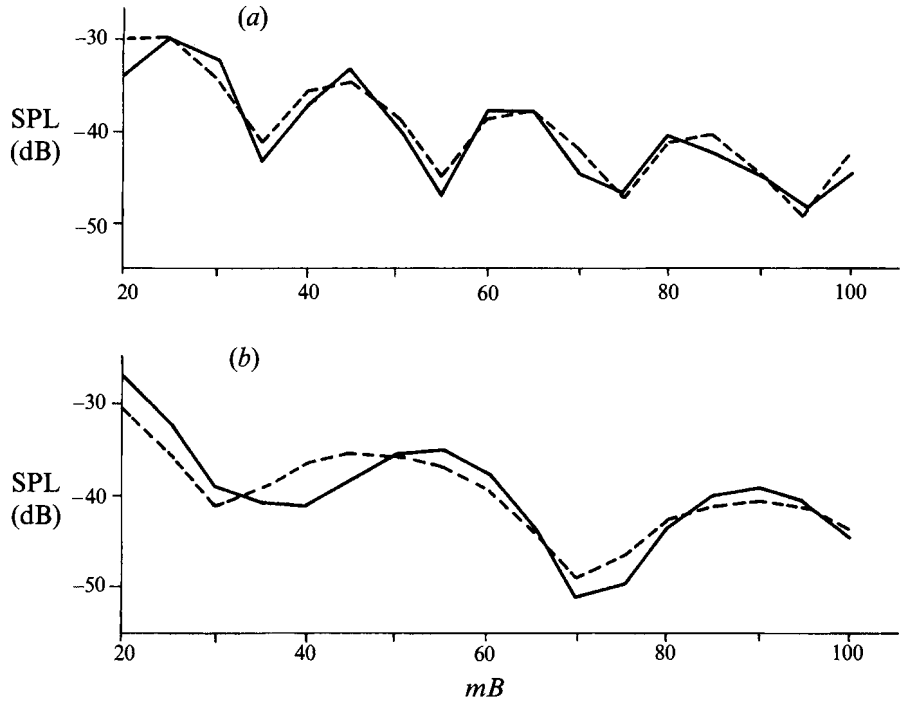

FIGURE 10. Comparison between numerical results and asymptotics for $20 \leqslant mB \leqslant 100$, $\lambda = 2$, parabolic leading edges: (*a*) $M_x = 0.8$, $M_t = 0.8$, $\theta = 37°$; (*b*) $M_x = 0$, $M_t = 1.2$, $\theta = 90°$.

regime $\lambda > 1$. In order to understand the reason for this increase we must recall that for $\lambda > 1$ the radiation comes mainly from the tip and is given, asymptotically, by (51). This equation represents the sum of two contributions from different azimuthal positions, i.e. the points at which the leading edge at the blade tip cuts the Mach plane on both the 'up stroke' and the 'down stroke' (see §5). Phase adding the radiation from these two points thus produces levels which oscillate with increasing mB but have envelope decay $(mB)^{-1}$ or $(mB)^{-3/2}$. Results of noise level against frequency (represented by mB) are shown in figure 10 for blunt leading-edge airfoil sections; parts (*a*) and (*b*) represent 'cruise' and 'take-off' conditions respectively. The interference pattern generated by the two tip sources is clearly illustrated. The different rates of oscillation in (*a*) and (*b*) are due to differences in the phase factor in the argument of the exponential in (75): using (1) with $\cos\theta = M_x$, and expanding the inverse tangent, the term in square brackets becomes $\frac{1}{3}[(M_{rt}^2 - 1)/(1 - M_x^2)]^{3/2}$, where M_{rt} is the tip helical Mach number; this factor takes twice the value at 'cruise' that it does at 'take-off'.

8. Conclusions

In this paper we have used an asymptotic frequency-domain approach, within the framework of linear theory, to predict and analyse the noise radiation from a swept propeller. Since the singular radiation originates from transonic rotor edges, a full understanding of the noise generation and radiation processes can only be obtained by including nonlinear effects (Hawkings & Lowson 1974; Tam & Salikuddin 1986). The present consensus, however, is that linear theory provides a good first approximation to the sound field, and that nonlinear effects result, mainly, in the truncation of

singularities down to finite size. In addition, most computer codes are still developed according to linear theory. It is, therefore, important that singularities arising from a linear acoustics approach are fully understood.

In the case of a propeller with a supersonic leading edge the radiation was found to be dominated by contributions from Mach radii (in agreement with the time-domain approach of Amiet 1988) – regions on the blade edges that move towards the observer at precisely sonic speed while at the same time having the edge normal to the line joining the source point and the observer – and the nature of singularities in the sound field is governed by details of blade edge shape and loading: a parabolic (blunt) leading edge produces an inverse square root and a wedge-shaped (sharp) leading edge produces a logarithm.

For a propeller with a completely subsonic leading edge we have shown that singularities can still be radiated from the tip; the singularities are due to a supersonic (tip) edge effect and, accordingly, are related to the blade edge details at the tip: a parabolic (blunt) leading edge at the tip produces both a pressure discontinuity (shock) and a logarithm.

Most importantly, we have shown that noise radiation can be substantially increased in certain directions, above that generated by a straight-bladed propeller, for a range of 'critical' sweep designs. Such designs have a continuous distribution of Mach radii along the blade edges with all of the singular radiation directed at the same observer point. Parabolic (blunt) leading edges result in both delta function and simple pole singularities; wedge-shaped (sharp) leading edges result in inverse square-root singularities. Both numerical and asymptotic results show that, at typical operating conditions, 'critical' designs are 5–10 dB noisier, in the direction of peak radiation, than straight-bladed designs. Although the noise radiation from a 'critical' design is reduced in off-peak directions (relative to straight-bladed designs), aircraft certification depends on effective perceived noise (EPN) levels which are dominated by radiation in the peak direction. It is, therefore, crucial to propeller designers that 'critical' designs are avoided.

Propeller designs which are similar, but not identical, to a 'critical' design – designs which have *nearly transonic* leading edges – can still encounter problems. A detailed discussion of transition through a critical design will, however, be presented elsewhere.

Once again, therefore, we have shown how a frequency-domain approach can display all of the characteristics of the acoustic field that can be obtained using a time-domain approach, such as the presence of singularities in the sound field and their points of origin on the propeller blades. In addition, the asymptotic analysis produces remarkably simplified, and accurate, solutions which enable us to pick out certain physical effects not immediately apparent from other approaches.

The author would like to thank Dr R. K. Amiet for his extremely helpful correspondence, particularly with regard to the *minimum sweep* designs discussed in §4.

Appendix

We use the polar coordinates (z, ϕ), where ϕ is related to t by $\phi = -t$, and the Cartesian coordinates (X, Y); the propeller disk is shown in figure 5. The blade leading-edge shape is given by (66) so that, from (10) and (22),

$$f(z,\phi) = -\phi + \frac{z}{z^*}\cos\phi - \left(\frac{z^2}{z^{*2}} - 1\right)^{1/2} + \tan^{-1}\left(\frac{z^2}{z^{*2}} - 1\right)^{1/2} \tag{A 1}$$

or, in Cartesian coordinates with $f(z,\phi) = F(X, Y)$,

$$F(X, Y) = \tan^{-1}\left(\frac{X}{Y}\right) + \frac{Y}{z^*} - \left(\frac{X^2+Y^2}{z^{*2}} - 1\right)^{1/2} + \tan^{-1}\left(\frac{X^2+Y^2}{z^{*2}} - 1\right)^{1/2}. \tag{A 2}$$

Differentiation produces

$$\frac{\partial F}{\partial Y} = \frac{-z^*X + X^2 + Y^2 - Y(X^2+Y^2-z^{*2})^{1/2}}{(X^2+Y^2)\,z^*}, \tag{A 3}$$

$$\frac{\partial F}{\partial X} = \frac{z^*Y - X(X^2+Y^2-z^{*2})^{1/2}}{(X^2+Y^2)\,z^*}, \tag{A 4}$$

from which we find that F has stationary points at $X = z^*$, for $0 < Y < (1-z^{*2})^{1/2}$, i.e. the stationary points lie on the intersection of the Mach plane with half of the nominal propeller disk plane (the section cut by a blade on the 'down stroke'). Since the integral (9) for harmonic pressure is dominated by the contributions from the stationary points as $mB \to \infty$ we find, on rewriting the integral in terms of X and Y and including non-compactness effects, that

$$P_m \sim \frac{1}{2\pi \mathrm{i}^{mB}} \int_{-\infty}^{\infty} \int_0^{(1-z^{*2})^{1/2}} \frac{S_L(z^{*2}+Y^2)^{1/2}}{(z^{*2}+Y^2)^{1/2}} \times \exp\left\{ imB\left[F(z^*, Y) + \frac{(X-z^*)^2}{2} \frac{\partial^2 F}{\partial X^2} F(z^*, Y) \right] \right\} \mathrm{d}Y\,\mathrm{d}X. \tag{A5}$$

From (A 2) and (A 4) we find that $F(z^*, Y) = \frac{1}{2}\pi$ and $\partial^2 F/\partial X^2\ (z^*, Y) = -1/(z^*Y)$ so that, evaluating the X-integral, we obtain

$$P_m \sim \left(\frac{z^*}{2\pi|mB|}\right)^{1/2} \mathrm{e}^{-\mathrm{i}\pi/4} \int_0^{(1-z^{*2})^{1/2}} \frac{Y^{1/2} S_L (z^{*2}+Y^2)^{1/2}}{(z^{*2}+Y^2)^{1/2}} \mathrm{d}Y. \tag{A 6}$$

The Y-integral here can easily be converted back to a z-integral using $z = (z^{*2}+Y^2)^{1/2}$ whence the result (67) follows.

REFERENCES

AMIET, R. K. 1988 Thickness noise of a propeller and its relation to blade sweep. *J. Fluid Mech.* **192**, 535–560.

BLEISTEIN, N. & HANDELSMAN, R. A. 1969 Uniform asymptotic expansions of double integrals. *J. Math. Anal. Appl.* **27**, 434–453.

CHAKO, N. 1965 Asymptotic expansions of double and multiple integrals occurring in diffraction theory. *J. Inst. Maths Applics.* **1**, 372–422.

CHAPMAN, C. J. 1988 Shocks and singularities in the pressure field of a supersonically rotating propeller. *J. Fluid Mech.* **192**, 1–16.

CRIGHTON, D. G. & PARRY, A. B. 1991 Asymptotic theory of propeller noise part II: supersonic single-rotation propeller. *AIAA J.* **29**, 2031–2037.

CRIGHTON, D. G. & PARRY, A. B. 1992 Higher approximations in the asymptotic theory of propeller noise. *AIAA J.* **30**, 23–28.

DINGLE, R. B. 1973 *Asymptotic Expansions: their Derivation and Interpretation.* Academic.

GRADSHTEYN, I. S. & RYZHIK, I. M. 1965 *Table of Integrals, Series, and Products.* Academic.

HANSON, D. B. 1980*a* Influence of propeller design parameters on far field harmonic noise in forward flight. *AIAA J.* **18**, 1313–1319.

HANSON, D. B. 1980*b* Helicoidal surface theory for harmonic noise of propellers in the far field. *AIAA J.* **18**, 1213–1220.

HAWKINGS, D. L. & LOWSON, M. V. 1974 Theory of open supersonic rotor noise. *J. Sound Vib.* **36**, 1–20.

JONES, D. S. & KLINE, M. 1958 Asymptotic expansions of multiple integrals and the method of stationary phase. *J. Math. Phys.* **37**, 1–28.

LIGHTHILL, M. J. 1958 *An Introduction to Fourier Analysis and Generalised Functions.* Cambridge University Press.

METZGER, F. B. & ROHRBACH, C. 1979 Aeroacoustic design of the propfan. *AIAA Paper* 79-0610.

METZGER, F. B. & ROHRBACH, C. 1985 Benefits of blade sweep for advanced turboprops. *AIAA Paper* 85-1260.

PARRY, A. B. & CRIGHTON, D. G. 1989 Asymptotic theory of propeller noise part I: subsonic single-rotation propeller. *AIAA J.* **27**, 1184–1190.

TAM, C. K. W. 1983 On linear acoustic solutions of high speed helicopter impulsive noise problems. *J. Sound Vib.* **89**, 119–134.

TAM, C. K. W. & SALIKUDDIN, M. 1986 Weakly nonlinear acoustic and shock-wave theory of the noise of advanced high-speed turbopropellers. *J. Fluid Mech.* **164**, 127–154.